Comparison of Two Convective/Stratiform Precipitation Classification Techniques: Radar Reflectivity Texture versus Drop Size Distribution–Based Approach

Guillaume Penide, Alain Protat, Vickal V. Kumar, Peter T. May

▶ **To cite this version:**

Guillaume Penide, Alain Protat, Vickal V. Kumar, Peter T. May. Comparison of Two Convective/Stratiform Precipitation Classification Techniques: Radar Reflectivity Texture versus Drop Size Distribution–Based Approach. Journal of Atmospheric and Oceanic Technology, 2013, Journal of Atmospheric and Oceanic Technology, 30 (12), pp.2788-2797. 10.1175/jtech-d-13-00019.1 . hal-04475177

HAL Id: hal-04475177
https://hal.univ-lille.fr/hal-04475177v1

Submitted on 27 Feb 2024

HAL is a multi-disciplinary open access archive for the deposit and dissemination of scientific research documents, whether they are published or not. The documents may come from teaching and research institutions in France or abroad, or from public or private research centers.

L'archive ouverte pluridisciplinaire **HAL**, est destinée au dépôt et à la diffusion de documents scientifiques de niveau recherche, publiés ou non, émanant des établissements d'enseignement et de recherche français ou étrangers, des laboratoires publics ou privés.

Comparison of Two Convective/Stratiform Precipitation Classification Techniques: Radar Reflectivity Texture versus Drop Size Distribution–Based Approach

GUILLAUME PENIDE

Laboratoire d'Optique Atmosphérique, UMR CNRS 8518, Université des Sciences et Technologies de Lille, Villeneuve d'Ascq, France

ALAIN PROTAT

Centre for Australian Weather and Climate Research, Melbourne, Victoria, Australia

VICKAL V. KUMAR

Centre for Australian Weather and Climate Research, Melbourne, and School of Mathematical Sciences, Monash University, Clayton, Victoria, Australia

PETER T. MAY

Centre for Australian Weather and Climate Research, Melbourne, Victoria, Australia

(Manuscript received 14 January 2013, in final form 16 August 2013)

ABSTRACT

C-band polarimetric radar measurements spanning two wet seasons are used to perform a critical evaluation of two algorithms for the classification of stratiform and convective precipitation. The first approach is based on the horizontal texture of the radar reflectivity field (two classes: stratiform, convective), and the second approach is based on the properties of the drop size distribution (DSD) parameters as derived from a set of polarimetric variables (three classes: stratiform, mixed, convective). To investigate how well those two methods compare quantitatively, probability density functions of reflectivity, rain rate, 5-dBZ echo top height, and DSD parameters (namely, the median volume diameter and the ''generalized'' intercept parameter) are built. The study found that while the two methods agree well on the identification of stratiform precipitation, large differences are obtained for convective rainfall. The texture-based approach seems to classify too many points as being of convective nature compared to the DSD-based method. Among the points that are classified as convective by the texture-based approach, 25% correspond to low concentration of relatively small particles associated with rain rates below 10 mm h^{-1}. This large proportion of unrealistically low convective rain rates is not produced by the DSD-based approach, which only classifies 4% of the convective points with rain rates below 10 mm h^{-1}. These points were found to be mainly isolated points embedded within stratiform precipitation and associated with low cloud-top height, suggesting a misclassification of the texture-based approach. Thus, to improve the statistics of the convective class, three modified equations of the peakedness criterion used in the radar-based algorithm are proposed to decrease the number of misclassified points.

1. Introduction

Numerous studies are dedicated to the classification of rain types into stratiform and convective parts using ground in situ measurements (e.g., Leary and Houze 1979; Tokay and Short 1996), ground radars (e.g., Williams et al. 1995; Steiner et al. 1995, hereafter SHY; Biggerstaff and Listemaa 2000; Ulbrich and Atlas 2002, 2007; Bringi et al. 2009, hereafter BAL; Thurai et al. 2010) or visible/infrared/microwave satellite data (e.g., Adler and Negri 1988; Anagnostou and Kummerov 1997; Hong et al. 1999). Convective and stratiform parts of cloud systems exhibit significant differences in terms of dynamics and, consequently, in terms of microphysics (Houze 1997). Indeed, vertical air motions within these

Corresponding author address: Guillaume Penide, Laboratoire d'Optique Atmosphérique, UMR CNRS 8518, Université Lille 1, 59655 Villeneuve d'Ascq CEDEX, France.
E-mail: guillaume.penide@univ-lille1.fr

DOI: 10.1175/JTECH-D-13-00019.1

© 2013 American Meteorological Society

Unauthenticated | Downloaded 02/27/24 03:05 PM UTC

two portions of a cloud system differ significantly; convective parts are mainly driven by large narrow updrafts (5–10 m s^{-1} or more), while stratiform portions are governed by gentler mesoscale ascents (<3 m s^{-1}). Thus, microphysical processes that drive the particle growth within the convective and stratiform parts are very different. Particles in convective cores mainly grow by riming or accretion (collection of liquid water droplets onto the ice particle surface), which leads to large/dense hydrometeors, whereas in the stratiform region, as vapor deposition and aggregation prevail, ice hydrometeors tend to be smaller (though large aggregates may exist) and particularly less dense, which once melted lead to smaller raindrops. Thus, it is important that different rain types be treated separately in order to extract consistent features, patterns, and conclusions about cloud processes. The approach considered in the present paper is to test two different methods: (i) the so-called Steiner's method, based on the texture of the radar reflectivity fields (e.g., SHY), which is widely used by the radar community; and (ii) a more recent approach based on the characteristics of the drop size distribution (DSD) as derived from a set of polarimetric variables (hence, only applicable to a dual-polarization radar), which is described in BAL. This paper builds on the prior work of Thurai et al. (2010), which aimed at testing the DSD-based approach against the SHY method on a 10-day dataset during the northern Australian monsoon. Herein, we extend the dataset to a total of 360 days distributed between two wet seasons (October–April in 2005–2006 and 2006–2007) using data from the C-POL radar (Keenan et al. 1998) located near Darwin, Australia. Note that both classification methods were originally built (and therefore are tuned) for the Darwin region and would need to be tested and tuned to other climate regions (other than the tropics) in order to extend the results presented herein to other regions. To extract consistent conclusions about each classification method and rain type, probability density functions (PDFs) of reflectivity (Z), rain rate (R), median volume diameter (D_0), and generalized intercept parameter (N_w) are built and then further compared in order to characterize, on a microphysical basis, which approach seems more realistic for defining the stratiform and convective classes.

2. C-POL radar and DSD retrievals

C-band polarimetric (C-POL) radar (Keenan et al. 1998) is a dual-polarized radar (5.5 GHz) located near Darwin, Australia. C-POL radar performs a volumetric scan of the surrounding atmosphere every 10 min within a radius of 150 km, using 15 elevation angles (from 0.5° to 43.1°) with azimuthal and radial resolutions of 1° and 300 m, respectively. On each of these 15 plan position indicator (PPI) scans, DSD parameters and rain rates are retrieved following BAL. In their paper, BAL developed an algorithm based on 6 months of disdrometer data to retrieve the median volume diameter (D_0 in mm) and the ''generalized'' intercept parameter (N_w in $mm^{-1} m^{-3}$) of a normalized gamma DSD (Testud et al. 2001) as well as the R (mm h^{-1}). Note that N_w is the same as the intercept parameter of an exponential DSD with the same D_0 and liquid water content as the gamma DSD. Inputs to this algorithm are the reflectivity factor at horizontal polarization (Z_h) and the differential reflectivity (Z_{dr}), which are corrected for a attenuation using the ZPHI method (Testud et al. 2000; Bringi et al. 2001) and the Tan et al. (1995) approach, respectively; and the specific differential phase (K_{dp}) derived from the differential propagation phase (Φ_{dp}) using the finite impulse response (FIR) range filter (Hubbert and Bringi 1995). Then, constant altitude plan position indicators (CAPPIs) at an altitude of 2.5 km are constructed by projection and interpolation of the radar data in polar coordinates onto a Cartesian grid with a horizontal resolution of 2.5 km × 2.5 km. Thus, each analysis is made at the same level, which avoids microphysical differences induced by altitude and possible contamination by ground clutter. Note that the scanning domain is about two-thirds land and one-third ocean, and that all types of convection (oceanic, coastal, continental) are used in the statistics.

3. Description of the two classification methods

a. Texture-based method (SHY)

The SHY method is based on the analysis of the horizontal gradient of the radar reflectivity field. This approach considers that any grid point within the radar scan radius, with reflectivity at least 40 dBZ or greater than a fluctuating threshold (peakedness criterion ΔZ) depending on the area-averaged background reflectivity (Z_{bg} calculated within a radius of 11 km around the grid point), is a convective center. In SHY ΔZ is given by

$$\Delta Z = \begin{cases} 10, & Z_{bg} < 0 \\ 10 - Z_{bg}^2/180, & 0 \le Z_{bg} < 42.43 \\ 0, & Z_{bg} > 42.43 \end{cases}. \quad (1)$$

Then, a radius of influence depending on the area-averaged background reflectivity is attributed to each convective center. This radius of influence (ranging from 1 to 5 km) is diagnosed using a simple step function described by an increase of the radius of influence of 1 km for every 5 dBZ in the range 20–40 dBZ (Fig. 6b in

Unauthenticated | Downloaded 02/27/24 03:05 PM UTC

SHY). Finally, all remaining nonzero reflectivities are classified as being stratiform.

b. DSD-based method (BAL)

BAL introduced a DSD-based classification technique with an additional third class defined as ''mixed'' rain or ''transition'' rain formed from decaying convective cells that have enough microphysical differences from purely stratiform and convective rain types to be considered as a (self-consistent) separated rain class (Williams et al. 1995). They showed that the inherent microphysical differences within the three regimes can be easily separated in the $\log_{10}(N_w)$–D_0 space using a simple linear function (separator criterion) given by

$$\log_{10}(N_w^{\text{sep}}) = -1.6D_0 + 6.3, \tag{2}$$

where D_0 is in millimeters, N_w is in millimeters per cubic meter, and the superscript sep stands for separator.

From this separator criterion, BAL built a simple index i, defined as the difference between the retrieved $\log_{10}(N_w^{\text{CPOL}})$ and Eq. (2):

$$i = \log_{10}(N_w^{\text{CPOL}}) - \log_{10}(N_w^{\text{sep}}), \tag{3}$$

such that large positive values refer to convective regions, large negative values represent stratiform regions, and $|i| < 0.1$ indicates transition regions. Notably, this classification method has been tested in Thurai et al. (2010) and used to build DSD parameter statistics according to various large-scale atmospheric environments in Penide et al. (2013).

4. Results: Convective/stratiform classifications

In the following, statistics of DSD parameters are compared according to the two classification methods. Two-sample Kolmogorov–Smirnov tests have been performed on each pair of PDFs to check their independency. This test gives 0 if the distributions are totally independent or 1 if the samples come from the same distribution. Values obtained with this test are all very close to zero (maximum value of about 10^{-5}), indicating that PDFs are independent. Considering the number of points used to build the statistics (between 2.2×10^5 and 2.3×10^7), small differences between the PDFs are also interpreted as being statistically significant (according to BAL). Moreover, BAL estimated the fractional error of D_0 to be around 9% and argued that considering the large number of points used to build their statistics (several thousands), the confidence interval in estimation of mean D_0 is much smaller than 0.116 mm, which represents the 1σ error. Thus, stratiform/mixed/convective precipitation are found to be distinct from both statistical and measurement uncertainty standpoints. Figure 1 presents PDFs of reflectivity, rain rates, and DSD parameters [namely, D_0 and $\log_{10}(N_w)$] corresponding to the SHY and BAL methods, which will be first analyzed separately and then further compared.

a. Texture-based method (SHY)

One can see in Fig. 1a that the 40-dBZ threshold has a clear signature on the PDF of convective reflectivities (discontinuity in the red curve). It appears that 37% of the convective points have reflectivity below 40 dBZ because of both the peakedness criteria and the radius of influence attributed to the convective centers. These low reflectivities have an important impact on the other PDFs, and notably on the rain-rate PDF (Fig. 1b), which exhibits a relatively large frequency of rain rates below 10 mm h^{-1} (i.e., 23% of the total convective points have $R < 10$ mm h^{-1}), which is the threshold often used to discriminate stratiform and convective precipitation (Leary and Houze 1979). Median values of the convective rain rate, D_0, and $\log_{10}(N_w)$ are 18.79 mm h^{-1}, 1.45 mm, and 4.1, respectively. And if we consider only the points with rain rates below 10 mm h^{-1}, then these median values fall to 1.20 mm for D_0 and 3.45 for $\log_{10}(N_w)$. Thus, these points correspond to low concentrations of relatively small particles. Long distribution tails at the lower end of both the D_0 and $\log_{10}(N_w)$ PDFs (Figs. 1c,d) probably correspond to misclassified points that are actually not of convective nature.

Stratiform PDFs are very different from the convective ones. The PDF of reflectivity is almost symmetrical (median value = 22.8 dBZ), with only 2.8% of points with rain rates above 10 mm h^{-1} and 90% with rain rates below 4.6 mm h^{-1}. Median values of D_0 and $\log_{10}(N_w)$ are 1.02 mm and 3.41, respectively, which corresponds to low concentrations of small hydrometeors. This is clearly what is expected for stratiform precipitation, except maybe the few points with rain rates larger than 10 mm h^{-1}.

b. DSD-based method (BAL)

First of all, it is obvious that the transition or mixed regime exhibits an intermediate behavior between the stratiform and convective PDFs (Fig. 1), which allows, as explained in Thurai et al. (2010), a smoother transition between those two regimes. The shape of the PDFs are very similar to the SHY method for stratiform rain, as well as median values: $Z = 22.7$ dBZ, $R = 0.70$ mm h^{-1}, $D_0 = 1.02$ mm, and $\log_{10}(N_w) = 3.41$. The main differences found between the two classification methods are for the convective PDFs. Indeed, in this case, only 20% of the points have reflectivities below 40 dBZ, which is

Unauthenticated | Downloaded 02/27/24 03:05 PM UTC

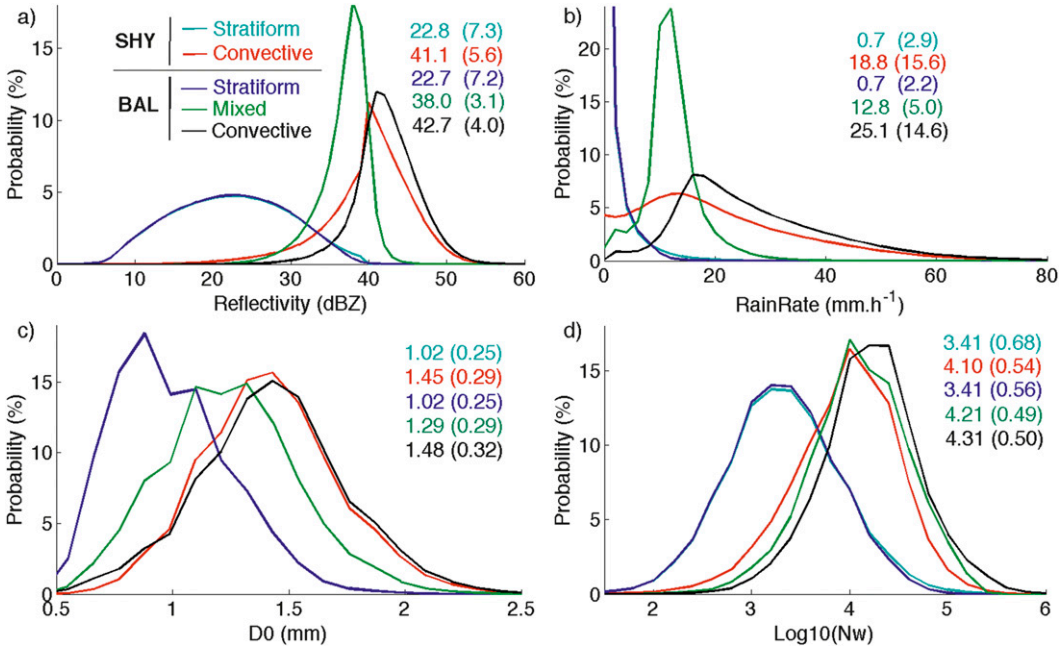

FIG. 1. PDFs of (a) reflectivity (dBZ), (b) rain rates (mm h^{-1}), (c) median volume diameter D_0 (mm), and (d) decimal logarithm of the generalized intercept parameter [$\log_{10}(N_w)$ with N_w (mm^{-1} m^{-3})] corresponding to the two classification methods (SHY and BAL). Light blue PDFs represent the SHY stratiform precipitation (2.28×10^7 points = 92.3% of the total), whereas red ones are relative to the SHY convective class (1.9×10^6 points = 7.7%). Dark blue PDFs are relative to the BAL stratiform class (2.28×10^7 points = 91.8%), green ones represent the mixed class (710 965 points = 2.8%), and black PDFs are associated with the BAL convective class (1.33×10^6 = 5.4%). Median values and standard deviations (brackets) corresponding to each PDF are also presented in each panel. Bins of 1 dBZ, 2 mm h^{-1}, 0.1 mm, and 0.2 have been used to build these PDFs.

much smaller than with the SHYmethod (37%). This lower percentage of low-reflectivity points within the convective class has an important impact on the resulting rainfall parameter PDFs. The percentage of convective points with rain rates below 10 mm h^{-1} drops from 23% with the SHY method to only 4% with the BAL approach. Consequently, median values of convective rain rates and $\log_{10}(N_w)$ strongly increase—R = 25.13 mm h^{-1} and $\log_{10}(N_w)$ = 4.31—while D_0 remains almost constant (from 1.45 mm with the SHY method to 1.48 with the BAL one). This indicates that the DSD-based classification removes the lower concentrations from the convective class, which is more consistent with previous studies of convective precipitation (Testud et al. 2001; Thurai et al. 2010). The mixed class represents only about 2.9% of the total number of points but acts to refine the convective class definition by mainly removing from the SHY convective class the high concentration of intermediate-size particles, which are associated with moderate rain rates [median values: Z = 38 dBZ, R = 12.75 mm h^{-1}, D_0 = 1.29 mm, and $\log_{10}(N_w)$ = 4.21]. These DSD characteristics could be encountered, for example, in young or decaying phases of deep convective events, shallow/weak convection or during the transition phase between convection, and stratiform precipitation. Thus, these various hypotheses make the definition of this mixed class wider than a simple transition class between convective and stratiform precipitation. In this context, an ''uncertain'' class situated between purely stratiform precipitation and mature/active convection seems to be a more suitable definition.

c. SHY versus BAL

Direct comparisons of the two methods have been carried out in Fig. 2, which shows pie charts representing how the SHY stratiform (Fig. 2a) and convective points (Fig. 2b) are classified when using the DSD-based method. First, about 4% (and 3%) of the data classified as being stratiform (convective) with SHY have no correspondence with the BAL method. These points have been rejected by additional data quality checks carried out as part of the BAL technique. Second, only about 2% of the SHY stratiform points (Fig. 2a) are classified as being mixed precipitation with BAL, and only few points (less than 1%) are classified as convective. So, concerning the stratiform precipitation classification, the two methods are in agreement, which is consistent with the PDF results. Concerning the SHY

Unauthenticated | Downloaded 02/27/24 03:05 PM UTC

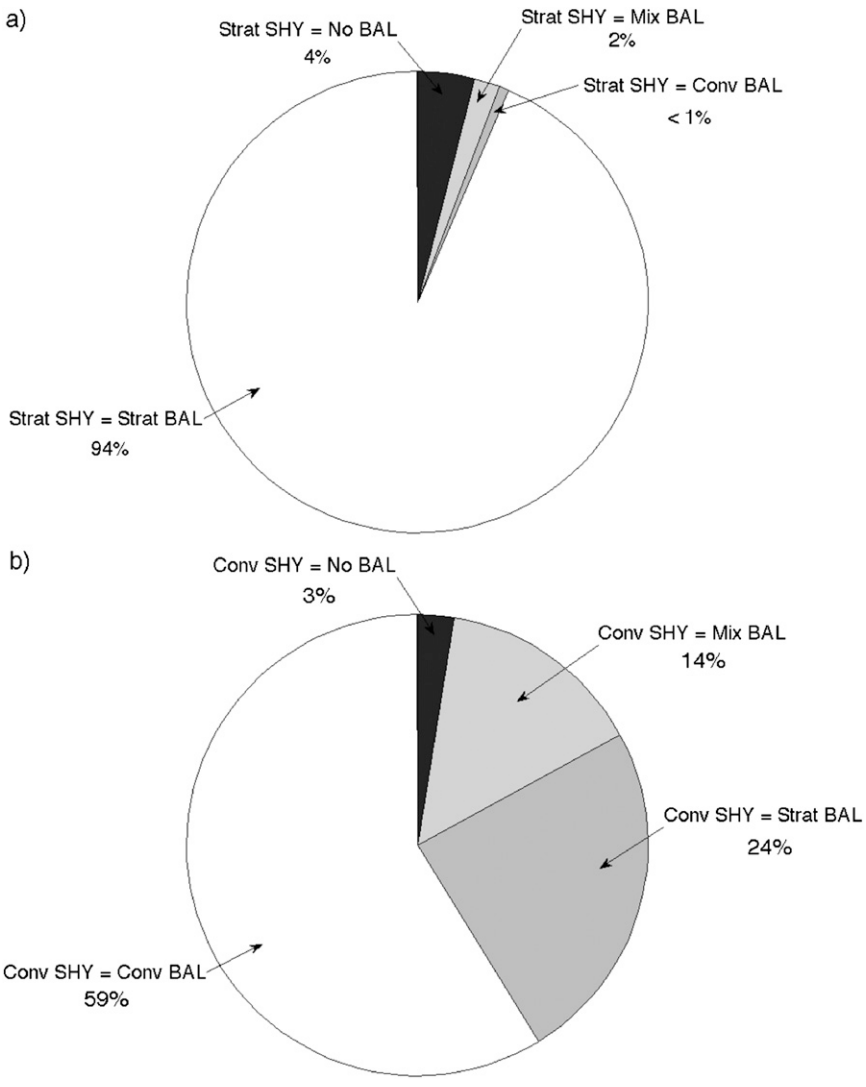

FIG. 2. Pie charts representing how the BAL classes (stratiform, mixed, and convective) are distributed among (a) the SHY stratiform class and (b) the SHY convective class.

convective points (Fig. 2b), it appears that only 55% of these points are classified as convective by the BAL's algorithm; 14% are classified as mixed and 24% are classified as being of stratiform nature with the DSD-based approach. This large disagreement explains, in part, the shape of the SHY convective PDFs (Fig. 1). Even though 14% of these SHY convective points falls into the mixed category, which seems realistic when looking at the SHY convective PDFs and which seemed to be the reason for the better performance of the BAL classification in a first step; we also found that almost one-fourth of SHY convective points have a stratiform-like DSD (i.e., low concentrations of relatively small raindrops associated with low rain rates), which is the major difference between the two classification schemes.

To characterize the microphysical properties of these points (Conv SHY = Strat BAL), PDFs corresponding to each of the BAL classes that are classified as being convective with the SHY method are analyzed (Fig. 3). Figure 3 highlights some of the previous points and clearly shows that 82% of the SHY convective points that are classified as stratiform with BAL (gray line in Fig. 3b) have rain rates below $10\,\mathrm{mm\,h^{-1}}$, which corresponds to pixels with reflectivity lower than 38 dBZ (Fig. 3a). These points are also characterized by low concentrations of small drops (Figs. 3c,d), which is very similar to the results found for the stratiform PDFs (Figs. 1c,d). Median values for the PDFs of these misclassified points are indeed situated between those of purely stratiform precipitation and those of the mixed

Unauthenticated | Downloaded 02/27/24 03:05 PM UTC

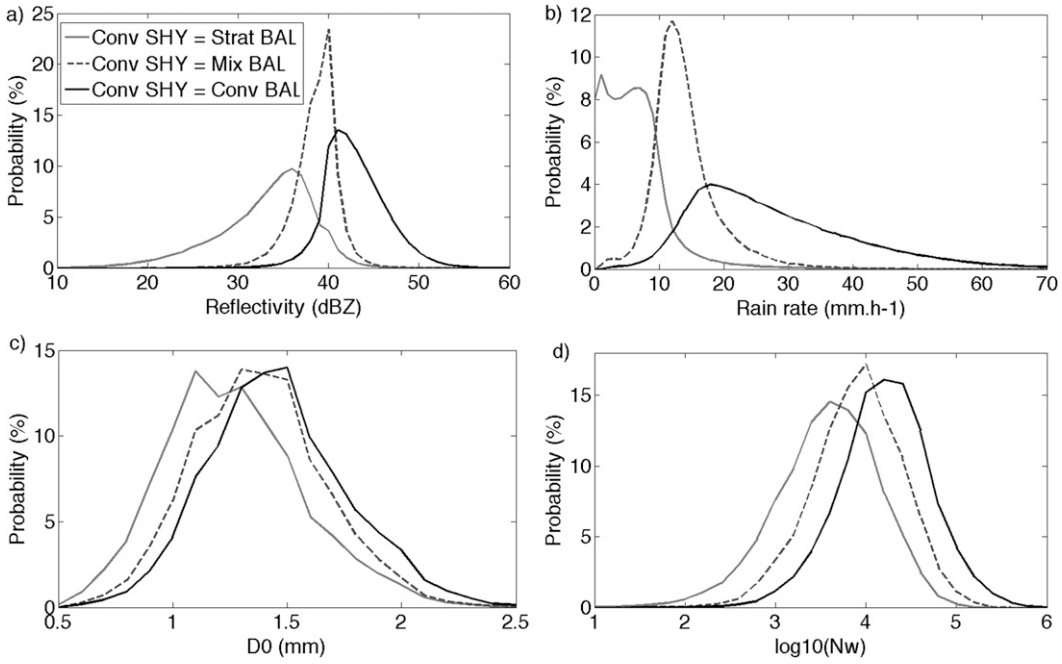

FIG. 3. As in Fig. 1, except that the PDFs correspond to the BAL classes (the gray line denotes stratiform, the dashed gray line denotes mixed, and the black line denotes convective) that are classified as being convective with SHY.

class: $Z = 34\,\mathrm{dB}Z$, $R = 6.0\,\mathrm{mm\,h^{-1}}$, $D_0 = 1.29\,\mathrm{mm}$, and $\log_{10}(N_w) = 3.69$. Moreover, 61% of these points have an index i [Eq. (3)] in the range $[-0.5; -0.1]$, whereas pure stratiform precipitation has only 10% of its points within the same range of values (i.e., closer to the $[-0.1; 0.1]$ range corresponding to the mixed or uncertain class). The microphysical characterization of these points (Fig. 3) therefore clearly suggests that they are indeed misclassified by the SHY method.

The BAL mixed category is characterized as expected by an intermediate behavior with intermediate concentrations of relatively large particles. When the two methods agree on convective precipitation, it clearly corresponds to active convection, as PDFs of reflectivity, DSD parameters, and rain rates are shifted toward larger values, and the percentage of rain rates below $10\,\mathrm{mm\,h^{-1}}$ falls to 2%. This category corresponds to about 92% of the BAL convective points. The remaining 8% of the BAL convective points could at first glance be considered as misclassified points, as they appear in the SHY stratiform class. However, half of these points are located within the tail of the SHY rain-rate PDF (i.e., with rain rate above $10\,\mathrm{mm\,h^{-1}}$).

This misclassification with the SHY approach appears even more pronounced (27% of disagreement Conv SHY = Strat BAL) when considering a data subset focusing on active monsoon periods (not shown) that is known to be a regime generating relatively small cell volumes that peak relatively low in altitude (Kumar et al. 2013). Thus, to check this result, PDFs of 5-dBZ echo tops corresponding to each of the convective pie chart sectors in Fig. 2b are presented in Fig. 4. One can easily see that the lower the echo tops, the higher the probability of misclassification with SHY. Indeed, the 50th (90th) percentile level of the echo top height is relatively low—8.5 (13.5) km—when the SHY convective points are classified as stratiform with BAL (gray PDF in Fig. 4) and it increases—to 10.5 (14.5) km—for the BAL mixed class (gray dashed line), and when the two methods agree with each other (black PDF), the median value reaches 12 (16) km. The reclassified points therefore seem to correspond, in part, to intermediate rainfall in the range $10–20\,\mathrm{mm\,h^{-1}}$ (tail of the gray line in Fig. 3b) associated with low echo tops, which is consistent with the definition of old/decaying convection but also with the definition of congestus clouds (Johnson et al. 1999). Nevertheless, statistics of the size of the misclassified points from the 2-yr dataset (not shown) indicate that these are mainly isolated points, as about 74% are made of only one point and in terms of cumulative distribution 99.4% are made of fewer than five points. Visual inspections of maps showing the two classification methods (a representative example is given in Fig. 5) confirm the previous results and also show that

Unauthenticated | Downloaded 02/27/24 03:05 PM UTC

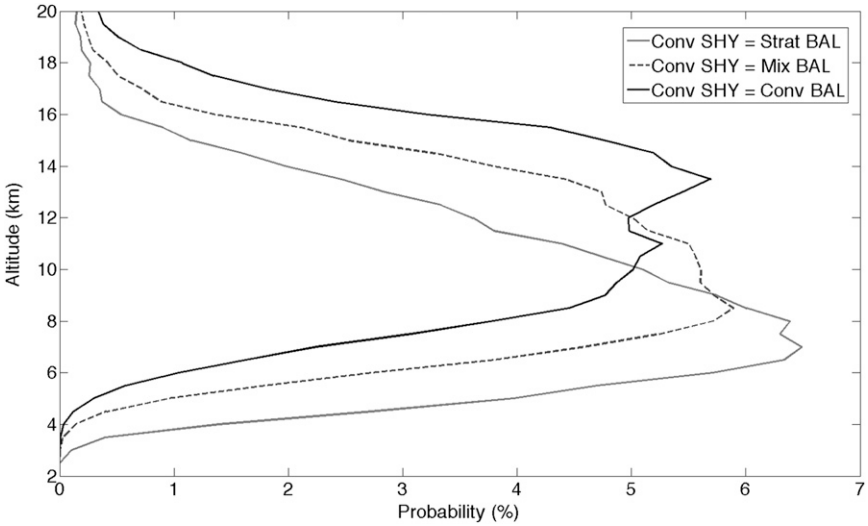

FIG. 4. PDF of 5-dBZ echo top relative to each of the BAL classes (the gray line represents stratiform, the dashed gray line represents mixed, and the black line represents convective) that are classified as being convective with the SHY method.

these misclassified points are in fact mainly isolated points embedded within stratiform areas.

Thus, the peakedness criterion used in the SHY method could be set higher than the actual threshold for such large stratiform area. This would avoid that precipitation coming from isolated old (and/or weak) convection (associated with slightly larger reflectivities than the background stratiform area) appearing in the same class as rainfall produced by active/vigorous convection. For example, within a stratiform precipitation area associated with a mean reflectivity of 20 dBZ, any point with at least a reflectivity factor of 27.7 dBZ will be classified as convective, such as the ones with reflectivities greater than 40 dBZ.

To investigate further this result, and in the aim of improving the SHY peakedness criterion, a 2D histogram representing the location of the misclassified points within the ΔZ–Z_{bg} space is shown in Fig. 6. One can easily see that the maximum density of the misclassified points is just above the original threshold [Eq. (1)] used in the SHY algorithm (i.e., the solid curve in Fig. 6). Indeed, the misclassified points are mainly situated between [20; 35] dBZ and within a range of [0; +2] dBZ above the original threshold. Thus, to improve the peakedness criterion so that the microphysical properties of the SHY convective points get closer to that of the BAL ones, various modified equations of the threshold have been tested (dashed curves in Fig. 6):

$$\Delta Z = 11 - (Z_{bg}^{2.05}/195), \tag{4}$$

$$\Delta Z = 12 - (Z_{bg}^{2.05}/180), \quad \text{and} \tag{5}$$

$$\Delta Z = 13 - (Z_{bg}^{2.05}/165). \tag{6}$$

These three modified equations were chosen so that the modified thresholds do not constrain too much the detection of convective precipitation within the high-reflectivity stratiform area (i.e., $Z_{bg} > 35$ dBZ) compared to the original threshold. We found that applying these new thresholds reduces the amount of misclassified points by 30% [Eq. (4)], 50% [Eq. (5)], and 64% [Eq. (6)], according to the desired level of constraint.

So, to conclude about the differences between these two methods and notably on the points that are convective for SHY and stratiform with BAL, these are mainly isolated points with low 5-dBZ echo tops and are associated with stratiform-like DSDs embedded within stratiform precipitation. Therefore, the use of DSD parameters retrieved from polarimetric radar measurements to classify precipitation and the introduction of a third class regrouping the uncertain points seems to provide a sound classification from a microphysical standpoint, while the texture-based method needs to be improved by applying one of the proposed peakedness criterion equations in order to provide a more robust classification of the convective points (i.e., closer to that given by the DSD-based method).

5. Conclusions

In this paper, a dataset of 2.5-km CAPPIs extracted from the C-POL radar measurements over two consecutive wet seasons has been used in order to compare two

Unauthenticated | Downloaded 02/27/24 03:05 PM UTC

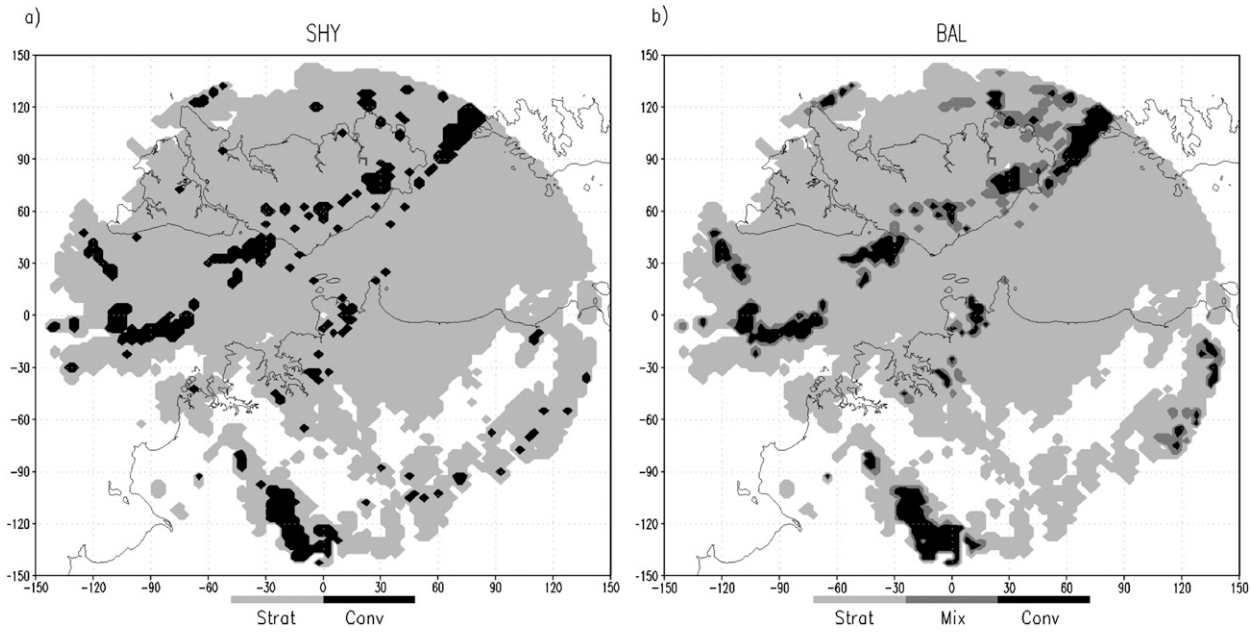

FIG. 5. Example of maps representing the results of the two classification methods at 1400 UTC 22 Jan 2006: (a) the SHY method and (b) the classification obtained with BAL. Axis labels are in kilometers and represent the distance from the radar that is located at (0; 0) coordinates.

precipitation classification methods. The aim was to characterize, from a microphysical standpoint, how these two methods accurately classify precipitation as being of stratiform or convective nature. To achieve this goal, PDFs of retrieved DSD parameters—rain rates (R), median volume diameter (D_0), and generalized intercept parameter (N_w)—have been built to analyze the statistical distribution of convective and stratiform classes.

Both methods agree well for stratiform cases. PDF shapes and the associated median values are very similar using both methods [in agreement with the results in Thurai et al. (2010)]. Less than 3% of stratiform rain rates are above the classical threshold of 10 mm h^{-1}, and 90% of all the stratiform points are associated with a rain rate below 4.6 mm h^{-1}, which corresponds, as expected for stratiform precipitation, to low concentrations of small drops.

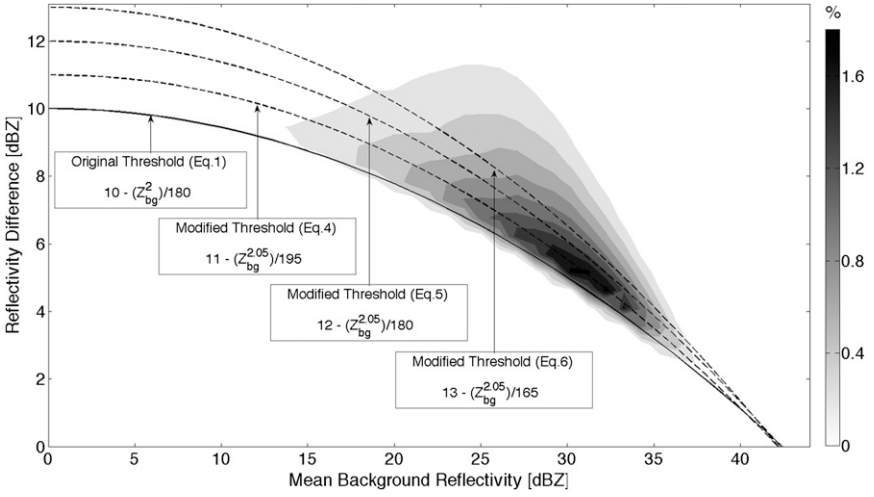

FIG. 6. Two-dimensional histogram representing the density of the misclassified points in the ΔZ–Z_{bg} space (i.e., the percentage of points per bin of background reflectivity and per bin of reflectivity difference between the grid point and the background reflectivity). The solid curve represents the original threshold used in the SHY algorithm, and the dashed curves represent the modified thresholds tested to improve the SHY convective class.

Unauthenticated | Downloaded 02/27/24 03:05 PM UTC

The main differences between these two very different approaches are found for the convective class. Indeed, SHY classifies many more points with rain rates below 10 mm h^{-1} as being of convective nature than the BAL method. This issue was found to be mostly due to the peakedness criterion and has an important impact on the PDFs and median values since, for example, the convective rain-rate median values increase of about 30% between the SHY method and the BAL method. One of the advantages of the BAL method is that it introduces a third precipitation class, which can be seen as a ''transition'' class between pure stratiform precipitation and mature/active convection. This transition class mainly contributes to refine the convective class definition, as 14% of SHY convective points fall into this category. This explains, in part, the better job of the BAL approach concerning the convective class. But, it appeared that almost one-fourth of the SHY convective points have a stratiform-like DSD, which is suggested to be a misclassification by the SHY method. So, the introduction of the ''uncertain'' class refines the BAL convective class, but the apparent misclassification of 24% of the convective points using the SHY method also increases the PDF differences. As shown with the 5-dBZ echo top PDF, this misclassification is correlated with cloud-top heights, since lower-topped clouds have DSDs different enough from deep convection that they might appear to be ''misclassified'' (these clouds increase the probability that SHY misclassifies convective points). Moreover, statistics of the size of the reclassified clusters and visual inspection of the images demonstrate that these are not only single points but mainly isolated points embedded within stratiform areas.

Although the use of polarimetric variables and a DSD-based classification approach seems to better classify purely convective and purely stratiform precipitation, the SHY method still has a lot of applicability for single-polarization radars. However, it can be improved by constraining the peakedness criteria so that isolated points do not stand out in the surrounding stratiform precipitation area and do not appear in the convective class. The modified peakedness criterion equations proposed in the present paper reduce significantly the number of misclassified points (by up to 64%) so that statistics of the SHY convective microphysical properties are closer to that given by the DSD-based approach. As mentioned previously, these results are for the Darwin area and such statistical analysis should be repeated in other places to generalize the conclusions.

Acknowledgments. Part of this work was supported by the U.S. Department of Energy Atmospheric Radiation Measurement Program. The authors would like to acknowledge the contributions of Michael Whimpey in supporting the Darwin observatory and data management, and Loris Foresti and the anonymous reviewers for providing helpful comments on the manuscript.

REFERENCES

Adler, R. F., and A. J. Negri, 1988: A satellite infrared technique to estimate tropical convective and stratiform rainfall. *J. Appl. Meteor.,* **27,** 30–51.

Anagnostou, E. N., and C. D. Kummerov, 1997: Stratiform and convective classification of rainfall using SSM/I 85-GHz brightness temperature observations. *J. Atmos. Oceanic Technol.,* **14,** 570–575.

Biggerstaff, M. I., and S. A. Listemaa, 2000: An improved scheme for convective/stratiform echo classification using radar reflectivity. *J. Appl. Meteor.,* **39,** 2129–2149.

Bringi, V. N., T. D. Keenan, and V. Chandrasekar, 2001: Correcting C-band radar reflectivity and differential reflectivity data for rain attenuation: A self-consistent method with constraints. *IEEE Trans. Geosci. Remote Sens.,* **39,** 1906–1915.

——, C. R. Williams, M. Thurai, and P. T. May, 2009: Using dual-polarized radar and dual-frequency profiler for DSD characterization: A case study from Darwin, Australia. *J. Atmos. Oceanic Technol.,* **26,** 2107–2122.

Hong, Y., C. D. Kummerov, and W. S. Olson, 1999: Separation of convective and stratiform precipitation using microwave brightness temperature. *J. Appl. Meteor.,* **38,** 1195–1213.

Houze, R. L., 1997: Stratiform precipitation in regions of convection: A meteorological paradox? *Bull. Amer. Meteor. Soc.,* **78,** 2179–2196.

Hubbert, J., and V. N. Bringi, 1995: An iterative filtering technique for the analysis of copolar differential phase and dual-frequency radar measurements. *J. Atmos. Oceanic Technol.,* **12,** 643–648.

Johnson, R. H., T. M. Rickenbach, S. A. Rutledge, P. E. Ciesielski, and W. H. Schubert, 1999: Trimodal characteristics of tropical convection. *J. Climate,* **12,** 2397–2418.

Keenan, T., K. Glasson, F. Cummings, T. S. Bird, J. Keeler, and J. Lutz, 1998: The BMRC/NCAR C-band polarimetric (C-POL) radar system. *J. Atmos. Oceanic Technol.,* **15,** 871–886.

Kumar, V. V., A. Protat, P. T. May, C. Jacob, G. Penide, S. Kumar, and L. Davies, 2013: On the effects of large-scale environment and surface types on convective cloud characteristics over Darwin, Australia. *Mon. Wea. Rev.,* **141,** 1358–1374.

Leary, C. A., and R. A. Houze Jr., 1979: Melting and evaporation of hydrometeors in precipitation from the anvil clouds of deep tropical convection. *J. Atmos. Sci.,* **36,** 669–679.

Penide, G., V. V. Kumar, A. Protat, and P. T. May, 2013: Statistics of drop size distribution parameters and rain rates for stratiform and convective precipitation during the north Australian wet season. *Mon. Wea. Rev.,* **141,** 3222–3237.

Steiner, M., R. A. Houze Jr., and S. E. Yuter, 1995: Climatological characterization of three-dimensional storm structure from radar and rain gauge data. *J. Appl. Meteor.,* **34,** 1978–2007.

Tan, J., J. W. F. Goddard, and M. Thurai, 1995: Applications of differential propagation phase in polarisation-diversity radars at S-band and C-band. *Ninth International Conference on Antennas and Propagation,* Vol. 2, Conf. Publ. 407, IEEE, 336–341.

Testud, J., E. Le Bouar, E. Obligis, and M. Ali-Mehenni, 2000: The rain profiling algorithm applied to polarimetric weather radar. *J. Atmos. Oceanic Technol.,* **17,** 322–356.

——, S. Oury, P. Amayenc, and R. A. Black, 2001: The concept of ''normalized'' distributions to describe raindrop spectra: A

Unauthenticated | Downloaded 02/27/24 03:05 PM UTC

tool for cloud physics and cloud remote sensing. *J. Appl. Meteor.,* **40,** 1118–1140.

Thurai, M., V. N. Bringi, and P. T. May, 2010: CPOL radar-derived drop size distribution statistics of stratiform and convective rain for two regimes in Darwin, Australia. *J. Atmos. Oceanic Technol.,* **27,** 932–942.

Tokay, A., and D. A. Short, 1996: Evidence from tropical raindrop spectra of the origin of rain from stratiform versus convective clouds. *J. Appl. Meteor.,* **35,** 355–371.

Ulbrich, C. W., and D. Atlas, 2002: On the separation of tropical convective and stratiform rains. *J. Appl. Meteor. Climatol.,* **41,** 188–195.

——, and ——, 2007: Microphysics of raindrop size spectra: Tropical continental and maritime storms. *J. Appl. Meteor. Climatol.,* **46,** 1777–1791.

Williams, C. R., W. L. Ecklund, and K. S. Gage, 1995: Classification of precipitating clouds in tropics using 915-MHz wind profilers. *J. Atmos. Oceanic Technol.,* **12,** 996–1012.

Unauthenticated | Downloaded 02/27/24 03:05 PM UTC